Multiple Unfolding Intermediates of Human Placental Alkaline Phosphatase in Equilibrium Urea Denaturation

Hui-Chih Hung and Gu-Gang Chang

Department of Biochemistry, National Defense Medical Center, Taipei, Taiwan, Republic of China

ABSTRACT Alkaline phosphatase is an enzyme with a typical α/β hydrolase fold. The conformational stability of the human placental alkaline phosphatase was examined with the chemical denaturant urea. The red shifts of fluorescence spectra show a complex unfolding process involving multiple equilibrium intermediates indicating differential stability of the subdomains of the enzyme. None of these unfolding intermediates were observed in the presence of 83 mM NaCl, indicating the importance of ionic interactions in the stabilization of the unfolding intermediates. Guanidinium chloride, on the other hand, could stabilize one of the unfolding intermediates, which is not a salt effect. Some of the unfolding intermediates were also observed in circular dichroism spectroscopy, which clearly indicates steady loss of helical structure during unfolding, but very little change was observed for the β strand content until the late stage of the unfolding process. The enzyme does not lose its phosphate-binding ability after substantial tertiary structure changes, suggesting that the substrate-binding region is more resistant to chemical denaturant than the other structural domains. Global analysis of the fluorescence spectral change demonstrated the following folding-unfolding process of the enzyme: $N \leftrightarrow I_1 \leftrightarrow I_2 \leftrightarrow I_3 \leftrightarrow I_4 \leftrightarrow I_5 \leftrightarrow D$. These discrete intermediates are stable at urea concentrations of 2.6, 4.1, 4.7, 5.5, 6.6, and 7.7 M, respectively. These intermediates are further characterized by acrylamide and/or potassium iodide quenching of the intrinsic fluorescence of the enzyme and by the hydrophobic probes, 1-anilinonaphthalene-8-sulfonic acid and 4,4′-dianilino-1,1′-binaphthyl-5,5′-disulfonic acid. The stepwise unfolding process was interpreted by the folding energy landscape in terms of the unique structure of the enzyme. The rigid central β-strand domain is surrounded by the peripheral α-helical and coil structures, which are marginally stable toward a chemical denaturant.

INTRODUCTION

Alkaline phosphatase (orthophosphoric monoester phosphohydrolase (alkaline optimum), EC 3.1.3.1) belongs to the α/β hydrolase fold family (Ollis et al., 1992). This is one of the most versatile and widespread protein folds known and represents a typical example of tertiary structure adopted by various enzymes during divergent evolution (Nardini and Dijkstra, 1999). Human alkaline phosphatase isoenzymes have attracted much interest because of their clinical implications (Fishman, 1990; McComb et al., 1979; Moss, 1992; Van Hoof and De Broe, 1994). Alkaline phosphatase from placenta is characteristic for its stability compared with the other types of mammalian isoenzymes (Fishman, 1990; McComb et al., 1979). The thermostable properties of the placental-type alkaline phosphatase versus the thermolabile properties of the liver-bone-kidney-type isoenzyme had been used as a clinical diagnostic tool to attempt to differentiate between these isoenzymes (PetitClerc, 1976). The structural basis for this differential conformational stability is unclear. More recently, the crystal structure of human placental alkaline phosphatase became available (Le Du et al., 2001) and provided a very good model to examine the molecular basis for the conformational stability of the placental alkaline phosphatase. This model may provide valuable information about the stabilization of a protein molecule in general.

Alkaline phosphatase from *Escherichia coli* is quite unique in that the enzyme undergoes continued slow structural annealing long after the return of enzyme activity (Subramaniam et al., 1995). We have characterized the chemical stability of the placental alkaline phosphatase in GdnHCl in which a stable unfolding intermediate was identified (Hung and Chang, 1998). To further characterize the unfolding intermediate of the placental enzyme, we examined the urea-induced unfolding process. More significant results were obtained in the present study because more intermediates were identified.

MATERIALS AND METHODS

Materials

Partially purified human placental alkaline phosphatase (type XVII) and 4-nitrophenyl phosphate were purchased from Sigma-Aldrich (St. Louis, MO). Concanavalin A-sepharose and Q-sepharose were purchased from Amersham Pharmacia Biotech (Uppsala, Sweden). Urea and guanidinium chloride (GdnHCl) were purchased from E. Merck (Darmstadt, Germany). Acrylamide and potassium iodide (KI) were purchased from Baker (Phillipsburg, NJ). 1-anilinonaphthalene-8-sulfonic acid (ANS) and 4,4′-dianilino-1,1′-binaphthyl-5,5′-disulfonic acid (bis-ANS) were purchased from Molecular Probes (Eugene, OR).

Enzyme preparation

The partially purified enzyme from Sigma-Aldrich was further purified according to the published procedure by passing through a concanavalin-A affinity column, followed by a Q-sepharose column (Chang et al., 1992). The purified enzyme was subjected to sodium dodecyl sulfate-polyacryl-

Received for publication 20 November 2000 and in final form 28 August 2001.

Address reprint requests to Professor Gu-Gang Chang, Department of Biochemistry, National Defense Medical Center, P.O. Box 90048-501 (Neihu), Taipei 114, Taiwan, ROC. Tel.: 886-2-8792-3100 ext. 18833; Fax: 886-2-8792-1544; E-mail: ggchang@ndmctsgh.edu.tw.

0006-3495/01/12/3456/16 $2.00

amide gel electrophoresis to examine the purity. A single protein band corresponding to molecular weight of ~60 kDa was observed in all cases. An absorption coefficient of $115 \times 10^3\ M^{-1}\ cm^{-1}$ at 280 nm was used for protein concentration determination. A molecular weight of 115,000 for the dimeric enzyme was used for calculation of enzyme concentration (Sakiyama et al., 1979).

Enzyme assay

The assay mixture contained 100 mM $NaHCO_3$-Na_2CO_3 buffer (pH 9.8), 10 mM $MgCl_2$, 10 mM 4-nitrophenyl phosphate, and an appropriate amount of enzyme in a total volume of 1 ml. The hydrolyzed product, 4-nitrophenolate anion, was continuously monitored at 30°C with a Lambda-3B spectrophotometer (Perkin-Elmer, Foster City, CA). The increase of absorbance at 410 nm was always colinear with time. An absorption coefficient of $18.3 \times 10^3\ M^{-1}\ cm^{-1}$ for the 4-nitrophenolate was used for the calculation of product concentration (Dawson et al., 1986).

Enzyme unfolding

In the chemical unfolding experiments, the enzyme was incubated with various concentrations of urea in Tris-acetate buffer (0.1 M, pH 7.5) at 30°C for 24 h. The process of enzyme unfolding was monitored by assaying the initial rate of the residual enzyme activity, the fluorescence spectrum, and the circular dichroism (CD) change. In the enzyme activity assays, control experiments were performed simultaneously with the same amount of denaturant added into the control cuvette where the enzyme was not preincubated with the denaturant; e.g., if the enzyme was denatured in 3 M urea, then the enzyme activity was assayed in the presence of 3 M urea. Residual enzyme activity (E_t/E_o) was plotted versus denaturant concentration, in which E_o and E_t are the enzyme activity in the control and experimental cuvettes, respectively.

For monitoring the refolding process, the enzyme denatured with 8 M urea was diluted with Tris-acetate buffer (0.1 M, pH 7.5) to lower urea concentration and the fluorescence spectrum taken after overnight incubation at room temperature (25°C).

Analysis of the unfolding curves of the unfolding process followed the procedure of Pace (1986) or Morjana et al. (1993), assuming a two-state or a three-state unfolding mechanism, respectively (see later section for more complex unfolding mechanisms).

Spectrofluorimetric analysis

Fluorescence spectra of the enzyme were monitored with a Perkin-Elmer LS-50B luminescence spectrometer at 30°C, and all spectra were corrected for the buffer absorption. The Raman spectrum of water was also corrected. The excitation wavelength was set at 280 or 295 nm, and the fluorescence emission spectra were scanned from 300 to 400 nm. The maximal peak of the fluorescence spectrum and the change of fluorescence intensity at 360 nm were used in monitoring the unfolding processes of the enzyme.

Spectropolarimetric analysis

The secondary structure of the enzyme was analyzed by monitoring the CD spectrum of the protein at 25°C in a Jasco J-810 spectropolarimeter at 205 to 245 nm under constant N_2 flush. A quartz cuvette with a 1-mm light path was used. For direct comparison, all enzyme solutions were adjusted to the same protein concentration (0.15 mg/ml). The absorption spectrum of the buffer or buffer plus urea solution was also recorded and was subtracted from the protein spectrum. All spectra were accumulated over seven repeated scans.

The secondary structure of the enzyme after equilibrium urea unfolding was estimated by CONTIN, SELCON, and CDSSTR methods with an expanded reference set (Sreerama and Woody, 2000).

Fluorescence quenching experiments

The details of the enzyme conformation were analyzed with quenching experiments. Quenching titrations with either acrylamide or KI were performed at 30°C by sequentially added aliquots of the concentrated quencher stock solution (6 M) to the enzyme solution. Sodium thiosulfate (0.1 mM) was added to the KI stock solution to prevent I_3^- formation. The excitation wavelength was set at 295 nm, and the fluorescence emission spectra were scanned from 300 to 400 nm. The integration area among 330 and 360 nm were used for data analysis.

The inner filter effect due to acrylamide absorption was corrected according to the method of Calhoun et al. (1983)

$$F_{corr} = F_{obs} 10^{\left(\frac{A_{ex} + A_{em}}{2}\right)} \quad (1)$$

in which F_{corr} and F_{obs} are the corrected and observed fluorescence, respectively; A_{ex} and A_{em} are the acrylamide absorptions at the excitation and emission wavelengths, respectively.

The fluorescence quenching data in the presence in acrylamide or KI were analyzed by fitting to the Stern-Volmer equation (Eftink and Ghiron, 1981):

$$F_o/F = 1 + K_{sv} \times [Q] \quad (2)$$

in which F_o and F are the fluorescence intensities in the absence or presence of the quencher, respectively. K_{sv} is the Stern-Volmer quenching constant, and $[Q]$ is the quencher concentration.

A double-quenching experiment was also performed to further explore the protein dynamics. The enzyme was denatured to various degrees by preincubating the enzyme with different concentrations of urea as stated in the previous section. An appropriate concentration of KI was added into the enzyme solution before titrating with acrylamide. The double-quenching data were calculated by fitting the data according to Somogyi et al. (1985):

$$\frac{F_{1,2}}{F_o} = \frac{\alpha}{1 + K_{1e}[\text{acrylamide}] + K_2[KI]} + \frac{\beta}{1 + K_{1i}[\text{acrylamide}]} + \gamma \quad (3)$$

in which F_o is the original protein intrinsic fluorescence intensity and $F_{1,2}$ is fluorescence intensity in the presence of both acrylamide and KI. α, β, and γ represent the fraction of exposed (external), buried (internal), and nonquenchable fluorophors, respectively. Collisional quenching constants, K_{1e} and K_{1i}, are characterized for the exposed and the buried fluorophors for the nonselective quencher, respectively; K_2 is characterized for the selective quencher KI, which is ionic in character and can only quench the exposed fluorophors.

ANS and bis-ANS binding measurement

The excitation wavelengths were set at 370 and 395 nm for ANS and bis-ANS, respectively, and we rechecked the extinction coefficient of ANS and bis-ANS. The inner filter effects were corrected by using extinction coefficients of $5620\ M^{-1}\ cm^{-1}$ at 370 nm for ANS or $17{,}100\ M^{-1}\ cm^{-1}$ at 395 nm for bis-ANS. The emission spectra were scanned between 400 and 600 nm upon the respective excitation. All measurements were corrected for the background intensity of the buffer. The appropriate dilution factors due to sequential addition of ANS or bis-ANS were also corrected.

For urea unfolding experiments, the concentrations of ANS and bis-ANS were fixed at 40 and 4.0 μM, respectively, and the fluorescence emission spectra were integrated between 420 and 560 nm upon excitation at 370 nm and 395 nm, respectively.

For ANS or bis-ANS titration experiments, ANS or bis-ANS stock solution was sequentially added to the assay mixture and the final concentration of ANS or bis-ANS was 41.3 or 8.3 μM, and the fluorescence

emission intensities at 515 or 500 nm were observed upon excitation at 370 and 395 nm, respectively. The data were analyzed according to a hyperbolic binding behavior.

$$\Delta F = \frac{\Delta F_{\max} K_d}{[L] + K_d} \tag{4}$$

where ΔF is the fluorescence intensity change, $[L]$ is the concentration of ANS or bis-ANS. The value of K_d indicates the binding affinity of ANS or bis-ANS for the enzyme, and $\Delta F_{\max}$ is the fluorescence emission maximum for the maximal number ligand (ANS or bis-ANS) binding.

Molecular weight determination by sucrose-density gradient ultracentrifugation

Sucrose solutions were prepared with buffers containing the respective concentration of urea. A total of 12-ml linear sucrose gradient (5 to ~20%) in a centrifuge tube was formed with a Haake-Buchler Auto Densi-Flow IIC gradient former. Placental alkaline phosphatase after equilibrium denaturation with different concentrations of urea was layered on the top of the tube and centrifuged at 6500 × *g* (SW 41 Ti rotor) for 19 h at 25°C in a Beckman L8–70 ultracentrifuge. The centrifuged solution was fractionated into 30 fractions with the same auto-flow apparatus and assayed for enzyme activity and protein concentration. Because all sucrose gradients contained a constant urea concentration, after fractionation each tube will have the same amount of urea in that particular experiment. In a separate tube, bovine serum albumin (molecular weight 67,000) and β-galactosidase (molecular weight 116,000) were used as molecular weight markers for the monomeric and dimeric enzymes, respectively.

Quantitative analysis for more complex unfolding-refolding process

The equations that describe the dependence of an observed structural signal thermodynamic parameters for a seven-state unfolding model shown in Scheme 1 has been derived

$$N \overset{K_1}{\longleftrightarrow} I_1 \overset{K_2}{\longleftrightarrow} I_2 \overset{K_3}{\longleftrightarrow} I_3 \overset{K_4}{\longleftrightarrow} I_4 \overset{K_5}{\longleftrightarrow} I_5 \overset{K_6}{\longleftrightarrow} D$$

Scheme 1

in which N and D are the native and denatured states, respectively. I_1 through I_5 are the various unfolding intermediates. K_1 through K_6 are the dissociation constants of the corresponding steps. The detailed derivation of the equation for a seven-state folding process is given elsewhere, assuming linear free energy changes theory (Santoro and Bolen, 1988). According to this established theory each unfolding step has the following relationship of the standard free energy changes:

$$\Delta G_i^o = \Delta G_i + m_i[\mathrm{D}] \tag{5}$$

in which ΔG_i is the free energy change of each step, m represents the dependence of the ΔG on denaturant concentration [D]. In terms of equilibrium constants, the following relationships hold.

$$K_i = \exp\left\{\frac{-(\Delta G_i^o - m_i[\mathrm{D}])}{RT}\right\} \tag{6}$$

in which R is gas constant and T is the absolute temperature in Kelvin. The overall equation that describes a complex folding-unfolding system like that shown in Scheme 1 is shown in Eq. 7.

$$y_{\mathrm{obs}} = \frac{\left(\begin{array}{l} Y_N + Y_{I_1}\exp\left[-\dfrac{(\Delta G_1^o - m_1[\mathrm{D}])}{RT}\right] + Y_{I_2}\exp\left[-\dfrac{(\Delta G_1^o - m_1[\mathrm{D}] + \Delta G_2^o - m_2[\mathrm{D}])}{RT}\right] \\ + Y_{I_3}\exp\left[-\dfrac{(\Delta G_1^o - m_1[\mathrm{D}] + \Delta G_2^o - m_2[\mathrm{D}] + \Delta G_3^o - m_3[\mathrm{D}])}{RT}\right] \\ + Y_{I_4}\exp\left[-\dfrac{(\Delta G_1^o - m_1[\mathrm{D}] + \Delta G_2^o - m_2[\mathrm{D}] + \Delta G_3^o - m_3[\mathrm{D}] + \Delta G_4^o - m_4[\mathrm{D}])}{RT}\right] \\ + Y_{I_5}\exp\left[-\dfrac{(\Delta G_1^o - m_1[\mathrm{D}] + \Delta G_2^o - m_2[\mathrm{D}] + \Delta G_3^o - m_3[\mathrm{D}] + \Delta G_4^o - m_4[\mathrm{D}] + \Delta G_5^o - m_5[\mathrm{D}])}{RT}\right] \\ + Y_D\exp\left[-\dfrac{(\Delta G_1^o - m_1[\mathrm{D}] + \Delta G_2^o - m_2[\mathrm{D}] + \Delta G_3^o - m_3[\mathrm{D}] + \Delta G_4^o - m_4[\mathrm{D}] + \Delta G_5^o - m_5[\mathrm{D}] + \Delta G_6^o - m_6[\mathrm{D}])}{RT}\right] \end{array}\right)}{\left(\begin{array}{l} 1 + \exp\left[-\dfrac{(\Delta G_1^o - m_1[\mathrm{D}])}{RT}\right] + \exp\left[-\dfrac{(\Delta G_1^o - m_1[\mathrm{D}] + \Delta G_2^o - m_2[\mathrm{D}])}{RT}\right] \\ + \exp\left[-\dfrac{(\Delta G_1^o - m_1[\mathrm{D}] + \Delta G_2^o - m_2[\mathrm{D}] + \Delta G_3^o - m_3[\mathrm{D}])}{RT}\right] \\ + \exp\left[-\dfrac{(\Delta G_1^o - m_1[\mathrm{D}] + \Delta G_2^o - m_2[\mathrm{D}] + \Delta G_3^o - m_3[\mathrm{D}] + \Delta G_4^o - m_4[\mathrm{D}])}{RT}\right] \\ + \exp\left[-\dfrac{(\Delta G_1^o - m_1[\mathrm{D}] + \Delta G_2^o - m_2[\mathrm{D}] + \Delta G_3^o - m_3[\mathrm{D}] + \Delta G_4^o - m_4[\mathrm{D}] + \Delta G_5^o - m_5[\mathrm{D}])}{RT}\right] \\ + \exp\left[-\dfrac{(\Delta G_1^o - m_1[\mathrm{D}] + \Delta G_2^o - m_2[\mathrm{D}] + \Delta G_3^o - m_3[\mathrm{D}] + \Delta G_4^o - m_4[\mathrm{D}] + \Delta G_5^o - m_5[\mathrm{D}] + \Delta G_6^o - m_6[\mathrm{D}])}{RT}\right] \end{array}\right)} \tag{7}$$

in which Y_i is the y_{obs} value of the folding intermediate at the corresponding plateau region.

For a six-state unfolding model, deleting the last term from denominator and numerator can derive a similar equation. The same procedure applies to other equilibrium models. All fitting works were performed on Macintosh G4/500 microcomputer with the Sigma plot 5.0 program.

RESULTS

Multiphasic unfolding of human placental alkaline phosphatase induced by urea

Fluorescence methods are sensitive in monitoring unfolding transitions of proteins (Eftink, 1994). When monitored by fluorescence emission spectrum shifting, human placental alkaline phosphatase showed multiple intermediate states during the urea-induced unfolding process (Fig. 1 *A*). In this process, the fluorescence wavelength gradually shifted from 327 to 357 nm upon excitation at 280 nm, which excites all aromatic amino acid residues. The increase of fluorescence intensity, however, did not reach a plateau even at urea concentration of 9.5 M, indicating the existence of residual structures from the placental enzyme at this high concentration of urea (Fig. 1 *C*).

The unfolding of placental enzyme by urea was concentration dependent at extremely low protein concentrations. The unfolding curves were almost identical for protein concentrations between 12.9 and 64.8 μg/ml (Fig. 1 *A*). Lower protein concentrations down to 3.9 μg/ml caused the enzyme to become more sensitive to urea. Significant differences of the red shifting of the curve was observed at a protein concentration of 3.9 μg/ml (Fig. 1 *A*), but less change for the fluorescence intensity was observed for protein concentrations ranging from 3.9 to 64.8 μg/ml (Fig. 1 *C*). Placental alkaline phosphatase is a homodimeric enzyme. Dissociation will be sensitive to protein concentration. If the enzyme did dissociate into two monomers at the 3.9 μg/ml protein concentration, the unfolding behavior of the monomer would still be multiphasic, as shown by open squares in Fig. 1 *A*.

The multiphasic unfolding phenomena were analyzed by computer fitting of the original data to a seven-state or a six-state unfolding model. The data from 12.9 and 64.8 μg/ml were combined in the global analysis for a seven-state model. The fitted residuals (Fig. 1 *B*) showed good distribution around the zero line, indicating an acceptable model. However, it should be mentioned that there are a total of 19 parameters to be fitted. Due to the complexity of the fitting equation and the limited data points, some of the fitted parameters (e.g., ΔG_3 and m_3) have very large fitting errors. We are thus reluctant to report these calculated thermodynamic parameters. On the other hand, the urea concentrations that caused one-half transition of each step ($[\text{urea}]_{0.5}$), calculated from $\Delta G_i/m_i$, are quite reasonable as judged visually. The $[\text{urea}]_{0.5}$ levels corresponding to the $N \leftrightarrow I_1$, $I_1 \leftrightarrow I_2$, $I_2 \leftrightarrow I_3$, $I_3 \leftrightarrow I_4$, $I_4 \leftrightarrow I_5$, and $I_5 \leftrightarrow D$ processes are 2.6, 4.1, 4.7, 5.5, 6.6, and 7.7 M, respectively. Among these, the $[\text{urea}]_{0.5}$ value of 4.7 M for the $I_2 \leftrightarrow I_3$ step has large fitting errors because of the very small plateau region around 4.5 M urea concentration. The data of 3.9 μg/ml were best described by a six-state model with $[\text{urea}]_{0.5}$ at 2.6, 4.0, 5.4, 5.6, and 7.1 M, for the $N \leftrightarrow I_1$, $I_1 \leftrightarrow I_2$, $I_2 \leftrightarrow I_3$, $I_3 \leftrightarrow I_4$, and $I_4 \leftrightarrow D$, respectively. Among these, the 5.4 M value for the $I_2 \leftrightarrow I_3$ is also questionable but may be equivalent to the same transition at $[\text{urea}]_{0.5} =$ 4.7 M, as observed at higher protein concentrations. The only missing one at lower protein concentrations thus could be the $I_4 \leftrightarrow I_5$ process at $[\text{urea}]_{0.5} = 6.6$ M, which might be related to the dissociation/reassociation process (see below).

The unfolding process monitored by fluorescence spectra was completely reversible at urea concentrations up to 8 M. When the 8 M urea-denatured enzyme was diluted up to 10-fold to various degrees, fluorescence spectra obtained were identical with those of the unfolding enzymes at that urea concentration (solid circles in Fig. 2 *A*). These results suggest that the same folding-unfolding pathway was followed.

Quite different results were obtained when the same enzyme solution was excited with 295 nm of UV light, which registers only the tryptophanyl fluorescence of the enzyme. The fluorescence wavelength shift was monophasic, but the fluorescence intensity change was multiphasic (Fig. 3). The noncoincidence of different structural probes strongly indicates the existence of intermediates in the folding-unfolding process. The unfolding curves measured by the fluorescence wavelength shift and the fluorescence intensity were analyzed by two-state and five-state unfolding processes, respectively. The urea concentration that causes half of the fluorescence wavelength shift, $[\text{urea}]_{0.5}$, was at 4.5 M. The $[\text{urea}]_{0.5}$ values for the fluorescence intensity change were estimated to be 1.7, 5.2, 6.3, and 7.5 M. Some of the reliable thermodynamic parameters for these unfolding processes are summarized in Table 1.

Intermediate form during the urea-induced unfolding of human placental alkaline phosphatase can be stabilized by guanidinium chloride but not by NaCl

We have demonstrated a GdnHCl-induced biphasic unfolding process of the enzyme and also ruled out a salt effect on that biphasic phenomenon (Fig. 2 *A*, inset graph) (Hung and Chang, 1998). The urea-induced multiphasic unfolding phenomenon of placental alkaline phosphatase changed to monophasic by adding NaCl (83 mM) into the enzyme solutions during urea denaturation (Fig. 2 *A*, open squares). In the presence of salt, the unfolding curve measured by the fluorescence intensity change shifted to the left compared with the unfolding curve of urea only (Fig. 2 *B*, open squares). This indicates that addition of NaCl destabilizes the enzyme. We then checked the effect of GdnHCl on the

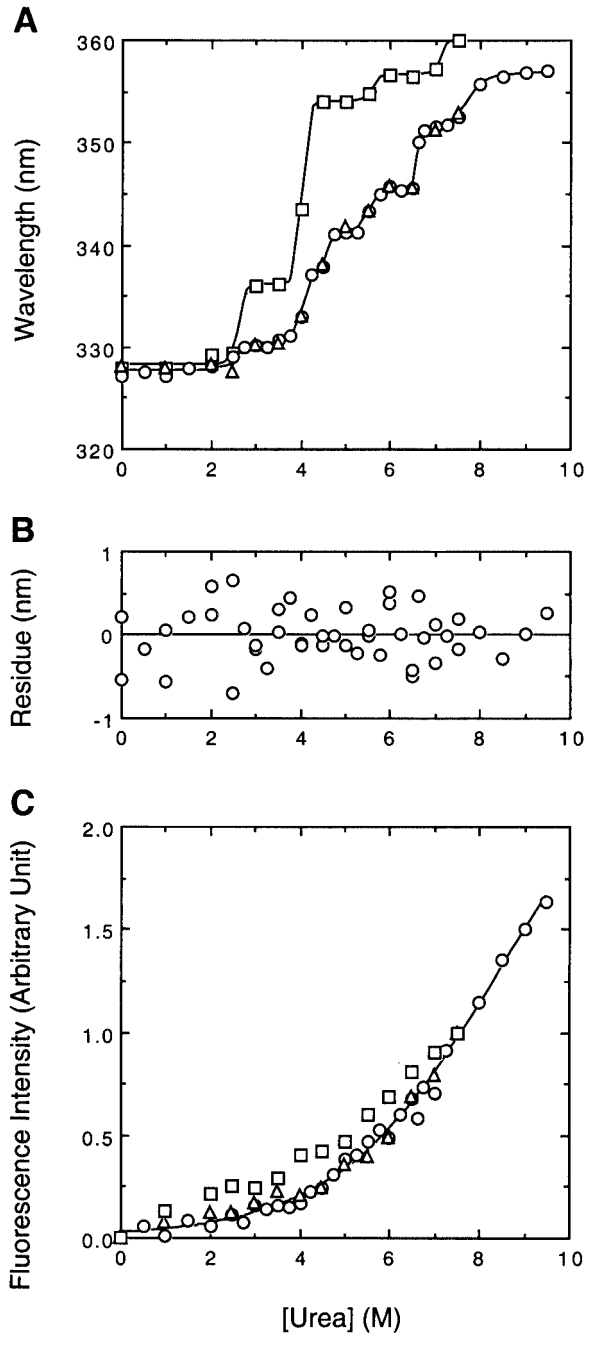

FIGURE 1 Multiphasic unfolding of human placental alkaline phosphatase induced by urea. Human placental alkaline phosphatase (△, 64.8 μg/ml; ○, 12.9 μg/ml; □, 3.88 μg/ml) in Tris-acetate buffer (0.1 M, pH 7.5) was unfolded with various concentrations of urea at 30°C for 24 h. The enzyme was excited at 280 nm and the fluorescence spectrum was recorded at 30°C. (*A*) Fluorescence emission maxima of the enzyme versus urea concentration. The symbols are experimental results, and the lines through these symbols are the computer fitted results according to a seven-state unfolding model for combined data from protein concentrations at 64.8 and 12.9 μg/ml, or according to a six-state unfolding model for protein concentration at 3.88 μg/ml. (*B*) Fitting residues for the seven-state unfolding model (combined data of protein concentrations at 64.8 and 12.9 μg/ml). Number of different repeating experiments ($N = 7$). (*C*) Fluorescence intensity ($\lambda = 360$ nm) of the denatured enzymes versus urea concentration. The same symbols are used as in *A*.

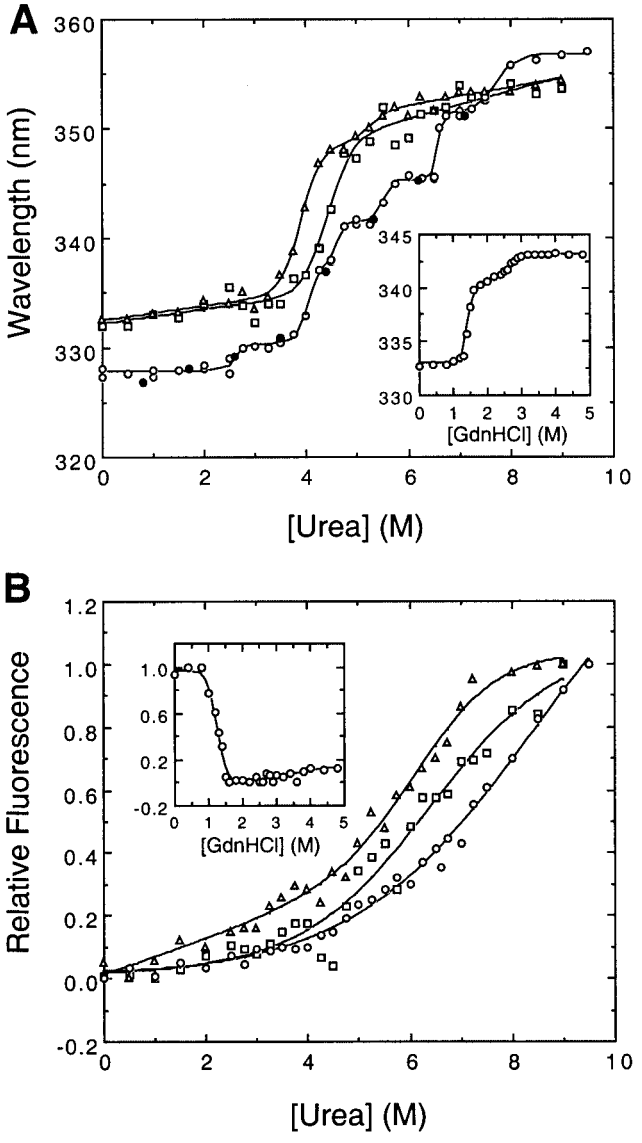

FIGURE 2 Effect of salt and guanidinium chloride on the fluorescence spectra of human placental alkaline phosphatase in the urea unfolding process. Human placental alkaline phosphatase (12.9 μg/ml) in Tris-acetate buffer (0.1 M, pH 7.5) was denatured with various concentrations of urea in the absence (○) and in the presence of 83 mM NaCl (□) or 83 mM GdnHCl (△). The excitation wavelength was set at 280 nm, and the fluorescence spectra were monitored between 300 and 400 nm. (*A* and *B*) Fluorescence wavelength shifting and the relative fluorescence intensities change at 360 nm, respectively. For comparison, the enzyme denatured by various concentrations of guanidinium chloride is shown in inset graphs of *A* and *B*. All the data were fitted according to two-state (□ in *A* and all curves in *B*), three-state (△ and *inset* curves in *A*), or seven-state unfolding mechanism (○ in *A*). The reversibility of the unfolding process was demonstrated by diluting the 8 M urea-denatured enzyme to lower urea concentrations with the enzyme concentration kept constant at 12.9 μg/ml (● in *A*) ($N = 2$).

urea unfolding. Biphasic unfolding of the placental enzyme was observed by addition of GdnHCl (83 mM) during urea unfolding (Fig. 2 *A*, open triangles). The unfolding curve for

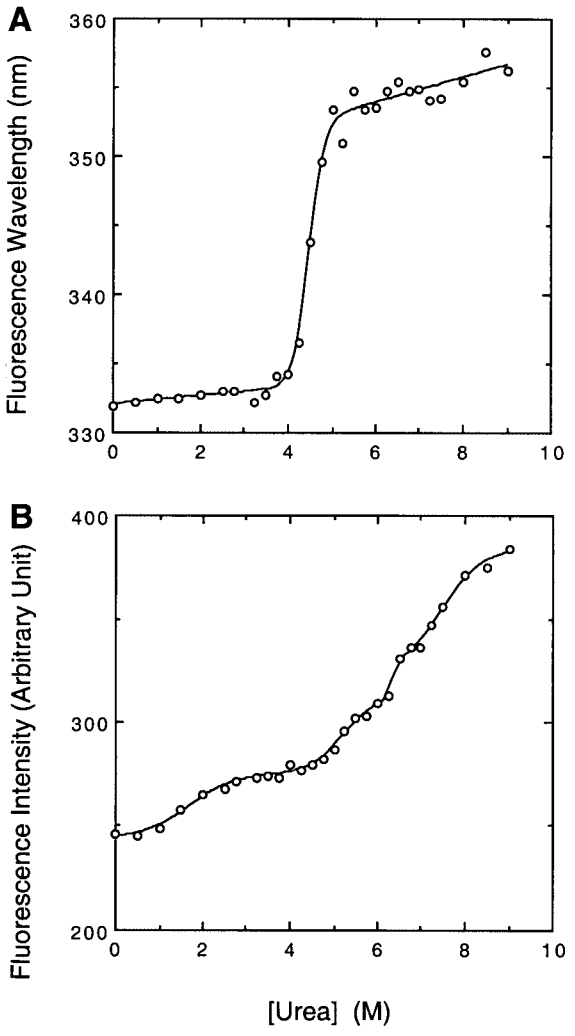

FIGURE 3 Tryptophan fluorescence in human placental alkaline phosphatase during urea unfolding process. Human placental alkaline phosphatase (12.9 μg/ml) in Tris-acetate buffer (0.1 M, pH 7.5) was denatured with various concentrations of urea at 30°C for 24 h. The enzyme was excited at 295 nm, and the fluorescence spectrum was recorded at 30°C. (*A*) Fluorescence emission wavelength versus urea concentration. (*B*) Fluorescence intensity (λ = 360 nm) versus urea concentration. The symbols are the experimental data and the lines are the computer fitting results according to a two- (*A*) or a five-state (*B*) model.

the fluorescence wavelength shift induced by urea plus GdnHCl was similar to that of the GdnHCl alone (Hung and Chang, 1998). Because 83 mM GdnHCl itself did not induce any unfolding of the enzyme (Hung and Chang, 1998), these results indicated that GdnHCl, but not NaCl, could help to entrap an unfolding intermediate and stabilize it during the unfolding process induced by urea. In the presence of GdnHCl, the $[\text{urea}]_{0.5}$ were estimated to be 3.9 and 5.2 M for the $N \leftrightarrow I_i$ and $I_i \leftrightarrow I_{i+1}$ processes, respectively. For the fluorescence intensity, data was fitted to a two-state transition, and the corresponding value of $[\text{urea}]_{0.5}$ was 6.3 M.

The unfolding curves for the fluorescence wavelength shift and fluorescence intensity changes in the presence of NaCl were fitted to the two-state transition separately. The corresponding values for $[\text{urea}]_{0.5}$ were 4.4 M for fluorescence wavelength shift, and 6.5 M for fluorescence intensity change, respectively, in the presence of NaCl.

Urea-induced multiphasic unfolding of human placental alkaline phosphatase detected by CD spectroscopy

Fig. 4 shows the equilibrium unfolding of human placental alkaline phosphatase monitored by CD at 222 nm. The relative CD signal change for the enzyme was best described by a four-state unfolding model during urea unfolding with three equilibrium $[\text{urea}]_{0.5}$ at ~0.4, 3.5, and 7.4 M, respectively (Fig. 4 *A*). Multiple intermediates seemed to be observed by adding 83 mM NaCl, however, all of these intermediates were destabilized by salt (Fig. 4 *B*), similar to those results on fluorescence (Fig. 2 *A*). One of these intermediates was stabilized by guanidinium chloride (83 mM) (Fig. 4 *C*), which was similar to the results observed from the fluorescence wavelength change (Fig. 2 *A*). GdnHCl itself induced a monophasic denaturation curve (Fig. 4 *D*). It is clear that multiple unfolding intermediates were also seen from the secondary structure change of the placental enzyme during the urea-induced unfolding process.

We then tried to correlate the CD signal to secondary structural changes of the enzyme. Prediction of secondary structure from the CD data varied considerably between different programs used. On the basis of known crystal structure of placental enzyme, we found that the program provided by Jasco was unreliable in protein secondary structure estimation. The recently published method (Sreerama and Woody, 2000) gave reasonably good estimations and was used in the present report. The helical contents of the unfolded enzyme decreased biphasically and monophasically, respectively, in the urea and GdnHCl denaturation (Fig. 5). The failure of helical contents to reveal more intermediates may be due to the insensitivity of the prediction programs. NaCl or GdnHCl can stabilize some of the helical structure in the urea-induced unfolding process (Fig. 5 *A*). The β strand structure, on the other hand, did not vary much until the very late stage of the denaturation process (data not shown).

Effect of urea on the kinetic parameters of human placental alkaline phosphatase

Human placental alkaline phosphatase was activated by low concentrations of urea but was denatured at high urea concentrations. The enzyme activity was ~1.2-fold higher than the native enzyme at 0.4 to 0.5 M urea. The activation and unfolding was a time-dependent process, indicating slow conformational changes at the active site of the protein. It

TABLE 1 Comparison of the conformational stability of the various unfolding intermediates of human placental alkaline phosphatase detected by different structural probes in urea unfolding process

Physical probes	$[Urea]_{0.5}$, (M)					
λ_{max} (Ex 280 nm) ([protein] $\geq$ 12.9 μg/ml)	2.6	4.1	4.7	5.5	6.6	7.7
λ_{max} (Ex 280 nm) ([protein] = 3.88 μg/ml)	2.6	4.0	5.4	5.6		7.1
λ_{max} (Ex 280 nm)* (in 83 mM NaCl)			4.4 (12 $\pm$ 2.8)†			
λ_{max} (Ex 280 nm) (in 83 mM GdnHCl)		3.9 (13 $\pm$ 1.8)		5.2 (17 $\pm$ 13)		
λ_{max} (Ex 295 nm)			4.5 (18 $\pm$ 2.7)			
F_{360} (Ex 280 nm)						8.5 (2.8 $\pm$ 0.2)
F_{360} (Ex 280 nm) (in 83 mM NaCl)					6.5 (3.0 $\pm$ 0.5)	
F_{360} (Ex 280 nm) (in 83 mM GdnHCl)					6.3 (4.8 $\pm$ 0.9)	
F_{360} (Ex 295 nm)	1.7 (2.0 $\pm$ 0.7)			5.2 (8.0 $\pm$ 2.4)	6.3 (98 $\pm$ 1.3)	7.5 (10 $\pm$ 3.2)
CD	0.4 (5.7 $\pm$ 0.9)	3.5 (5.3 $\pm$ 1.2)				7.4 (7.2 $\pm$ 1.1)
CD (in 83 mM GdnHCl)		4.1 (12 $\pm$ 5.1)				7.3 (14 $\pm$ 1.8)
Enzyme activity		3.9 (6.9 $\pm$ 2.8)			6.5 (1.8 $\pm$ 0.7)	
ANS binding		3.1 (4.4 $\pm$ 1.7)			6.1 (6.3 $\pm$ 2.0)	
Bis-ANS binding‡	0.8 (3.5 $\pm$ 1.0)		4.3 (1.7 $\pm$ 0.7)			
Bis-ANS binding§	1.0 (1.4 $\pm$ 0.6)				6.0 (8.4 $\pm$ 1.0)	

*Starting from this row, the protein concentration was 12.9 μg/ml.
†The numbers in parentheses are the free energy changes (ΔG in kcal/mol) calculated by fitting the results to the corresponding equations.
‡From area integration data.
§From maximum fluorescence emission wavelength data.

took at least a 24-h incubation for the enzyme activity change to reach equilibrium. The unfolding curve for enzyme activity change followed a three-state unfolding model (Fig. 6 *A*, open circles).

The inactivated enzyme activity was completely reversible up to 6 M urea (Fig. 6 *A*, closed circles). Higher urea concentrations caused partial reversibility of the enzyme activity. The change of k_{cat} values versus urea concentration showed a biphasic pattern (Fig. 6 *B*), similar to that shown in Fig. 6 *A*. On the other hand, the Michaelis constant for the substrate, 4-nitrophenyl phosphate was not changed at all in the urea concentrations tested (Fig. 6 *C*). These results indicate a rigid structure of the enzyme at the substrate-binding region.

Exploration of the structural dynamics of human placental alkaline phosphatase during urea unfolding by fluorescence-quenching experiments

Human placental alkaline phosphatase contains four tryptophan residues, and each tryptophan residue was characterized by its unique microenvironmental properties. Depending on their location in the protein matrix, they may be exposed to the solvent to various degrees. Quenching experiments were performed to detect the fluctuations of tryptophan residues in the placental alkaline phosphatase during the unfolding process. Acrylamide, a nonionic and a nonselective quencher, was able to penetrate the protein matrix and to quench the fluorescence of both exposed and buried tryptophan residues in proteins (Calhoun et al., 1983). In contrast, KI, a selective ionic quencher, could only quench the fluorescence of exposed tryptophan residues located at or near the protein surface (Lehrer, 1971).

More recently, Dobryszycki et al. (1999) have demonstrated that high concentrations of acrylamide induces time-dependent unfolding of rabbit muscle aldolase, which involves several intermediate states. In our case, the acrylamide concentration used was only up to 0.4 M, and the fluorescence quenching was measured immediately after adding the quencher. The use of acrylamide for analysis of the microenvironment of enzyme fluorophors induced by conformational changes of the enzyme should be safe (Lakowicz, 1999).

The data for the acrylamide and KI quenching of the native and denatured placental alkaline phosphatase were calculated according to the Stern-Volmer equation (Eq. 2). The slopes of the fitted lines, which represent the Stern-Volmer collisional quenching constants (K_{sv}) ascended with an increase of urea concentration indicating exposure of tryptophan residues during protein unfolding process (Fig. 7). Because of the red shifting of the fluorescence spectrum during enzyme unfolding, the quenching data were based on the integrated area between 330 and 360 nm. The K_{sv} values for KI quenching were smaller than those for acrylamide. The K_{sv} values of native and 8 M urea-denatured enzymes were 3.47 $\pm$ 0.06 M^{-1} and 7.74 $\pm$ 0.05 M^{-1} for acrylamide quenching, and 0.69 $\pm$ 0.01 M^{-1} and 1.90 $\pm$ 0.24 M^{-1} for KI quenching, respectively. The K_{sv} values versus urea concentration for acrylamide and KI quenching were shown in Fig. 7 *C*.

A double-quenching experiment was performed to further characterize the solvent-exposed and solvent-masked fluorophors during unfolding of the placental enzyme, and the

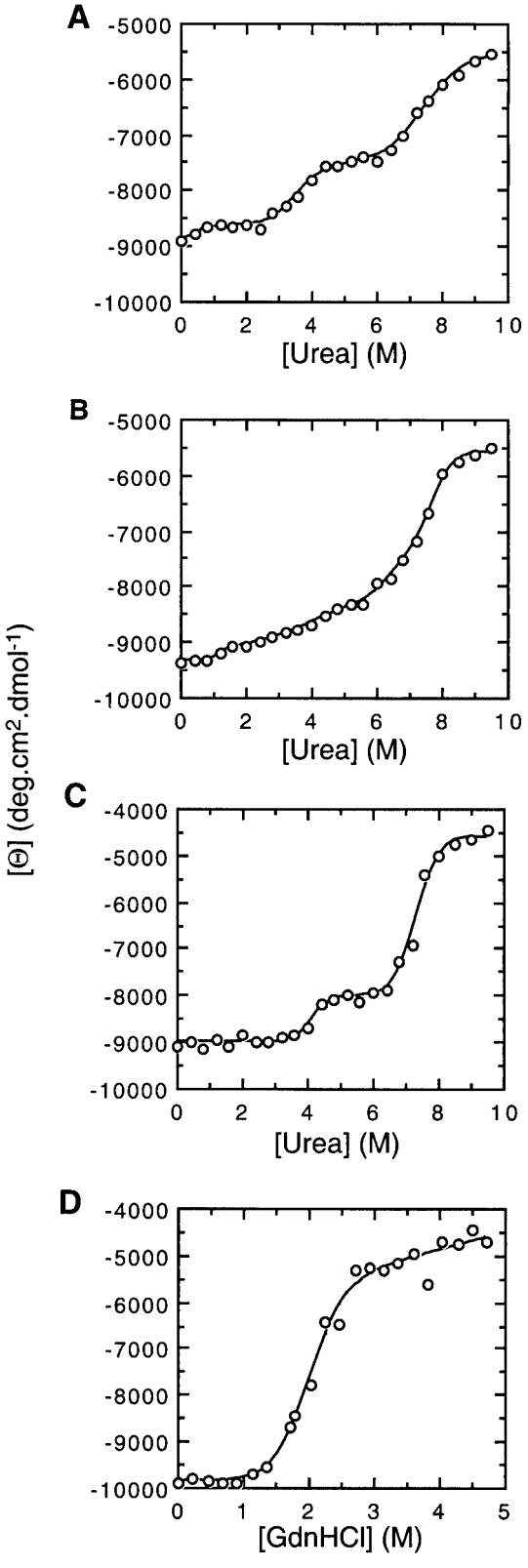

FIGURE 4 Changes of molecular ellipticity of human placental alkaline phosphatase in the urea unfolding process. Human placental alkaline phosphatase (0.15 mg/ml) in Tris-acetate buffer (0.1 M, pH 7.5) was denatured with various concentrations of urea in the absence (*A*) and in the presence of 83 mM NaCl (*B*) or 83 mM GdnHCl (*C*). Molecular ellipticity at 222 nm was used to monitor the enzyme structural changes. (*D*) Enzyme denatured by various concentrations of guanidinium chloride. The curves in *A* and *B* were fitted to a four-state or a five-state unfolding mechanism, respectively; whereas the data of *C* and *D* were fitted to a three-state or a two-state unfolding mechanism, respectively ($N = 2$).

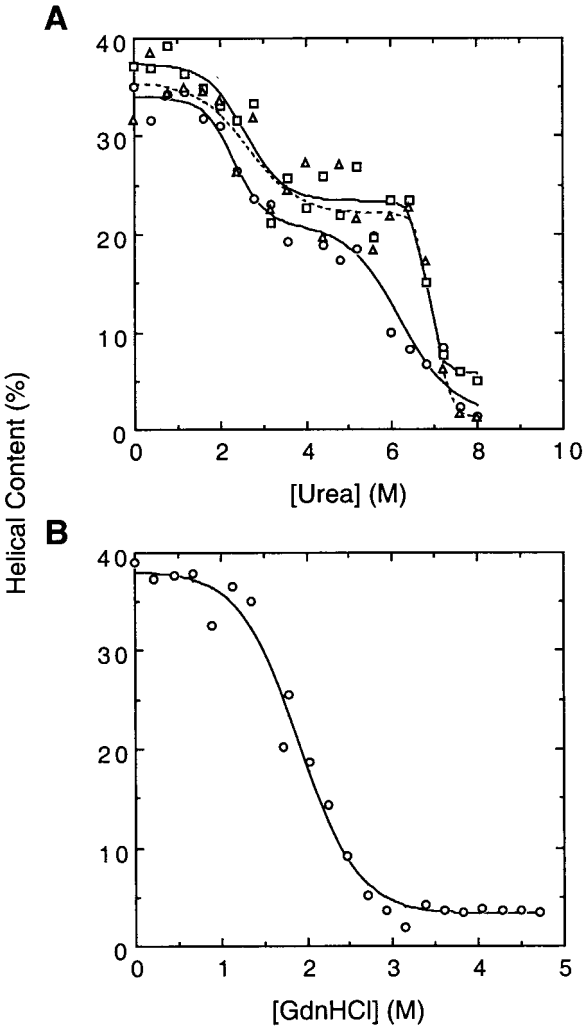

FIGURE 5 Helical contents of the human placental alkaline phosphatase during the urea unfolding process. The data shown in Fig. 4 were used in secondary structure estimation. Helical contents of the enzyme denatured with urea at various levels were estimated by CD spectra using the programs CONTIN, SELCON, and CDSSTR (Sreerama et al., 2000). (*A*) Human placental alkaline phosphatase denatured with urea in the absence (○) and in the presence of 83 mM NaCl (□) or 83 mM GdnHCl (△). (*B*) The same amount of enzyme denatured in GdnHCl.

experimental details are described in the Materials and Methods section. The double-quenching data were analyzed according to Eq. 3 (Somogyi et al., 1985). The primary plots gave a reasonable good fit (data not shown). The final fitting results are shown in Fig. 8. It can be seen that collisional quenching constants of the internal (K_{1i}) fluorophors for

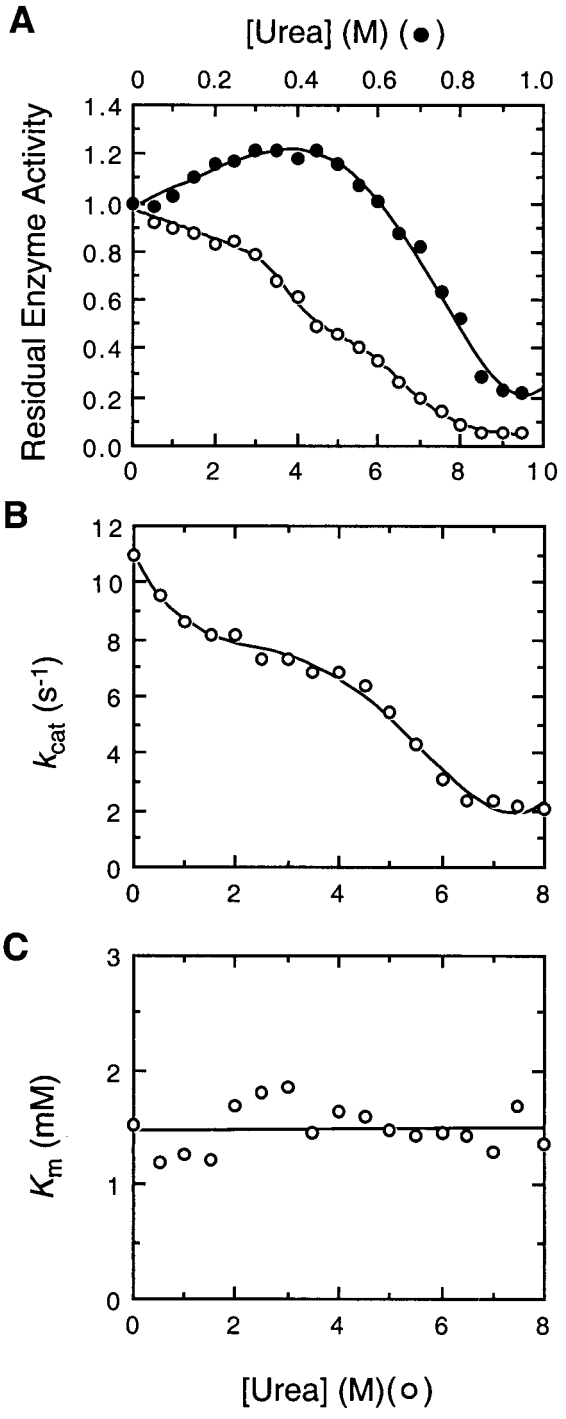

FIGURE 6 Effect of urea on the enzymatic activity of human placental alkaline phosphatase. (*A*) The enzyme (12.9 μg/ml in Tris-acetate buffer, 0.1 M, pH 7.5) was denatured with various concentrations of urea at 30°C for 24 h. The enzyme activity was then assayed at 30°C without (●) or with (○) the corresponding concentration of urea in the assay mixture. For those without addition of urea in the reaction mixture, the final urea concentration was diluted 10-fold in the assay mixture. (*B* and *C*), k_{cat} and K_m (4-nitrophenyl phosphate) versus urea concentration plots. The kinetic parameters of the partially denatured enzyme were determined at various concentrations of the substrate with the corresponding concentration of urea added in the assay mixture ($N = 2$).

acrylamide increased but not the external (K_{1e}) and collisional quenching constant for KI (K_2) with the denatured enzyme (Fig. 8 *B*). The fractions of exposed (α) and buried (β) tryptophan residues in the native placental enzyme were ~0.3 and ~0.6, respectively, which changed to ~0.8 and ~0.2 for the 7 M urea-denatured enzyme. There were ~10% non-quenchable (γ) fluorophors in the native enzyme. The quenching parameters, α and β versus concentration of urea seemed to follow a monophasic curve (Fig. 8 *A*). However, due to the limited data points and large errors, no further quantitative analysis was performed.

Detection of unfolding intermediates of human placental alkaline phosphatase by ANS and bis-ANS binding during urea-induced denaturation

ANS and bis-ANS are fluorescent compounds that have the ability to bind with hydrophobic areas on a protein molecule. Thus, they are excellent probes to detect unfolding intermediates, which usually involve exposure of internal hydrophobic areas.

ANS and bis-ANS exerted opposite binding behavior with the placental alkaline phosphatase. The ANS fluorescence increased at increasing urea concentration, indicating that ANS preferred binding to the denatured enzyme rather than to the native enzyme (Fig. 9 *A*). The maximal emission wavelength at 515 nm of ANS did not change upon urea unfolding. In contrast, bis-ANS fluorescence decreased at increasing urea concentration, and the fluorescence wavelength changed biphasically from 498 to 518 nm, reaching a plateau at ~503 nm between 2 to 5 M urea and then undergoing another change above 6 M urea (Fig. 9 *B*). The integrated fluorescence area also showed a biphasic process.

The unfolding curves measured by ANS and bis-ANS fluorescence were fitted to a three-state unfolding model to estimate the corresponding thermodynamic parameters (Table 1). The $[\text{urea}]_{0.5}$ values, corresponding to the $N \leftrightarrow I_i$ and $I_i \leftrightarrow I_{i+1}$ processes monitored by the ANS binding, were estimated to be 3.1 and 6.1 M, respectively. For the bis-ANS fluorescence intensity change, the corresponding values were 0.8 and 4.3 M, respectively. For the red shifting of bis-ANS fluorescence, the corresponding values of $[\text{urea}]_{0.5}$ were 1.0 and 6.0 M, respectively (Table 1).

Titration of the native- or denatured-enzyme with ANS and bis-ANS gave series of hyperbolic curves (data not shown). The titration curves were calculated according to a saturation phenomenon (Eq. 4) to estimate the apparent dissociation constants (K_d) between enzymes and ANS/bis-ANS (Table 2). The results clearly indicated that ANS molecules have stronger binding affinity to the denatured enzyme than to the native enzyme because the K_d values for the enzyme-ANS complex progressively decreased as the enzyme was gradually denatured. The dissociation constants for the ANS bound to the native enzyme and to the 8 M urea-denatured enzyme were 165.4 and 111.7 μM, re-

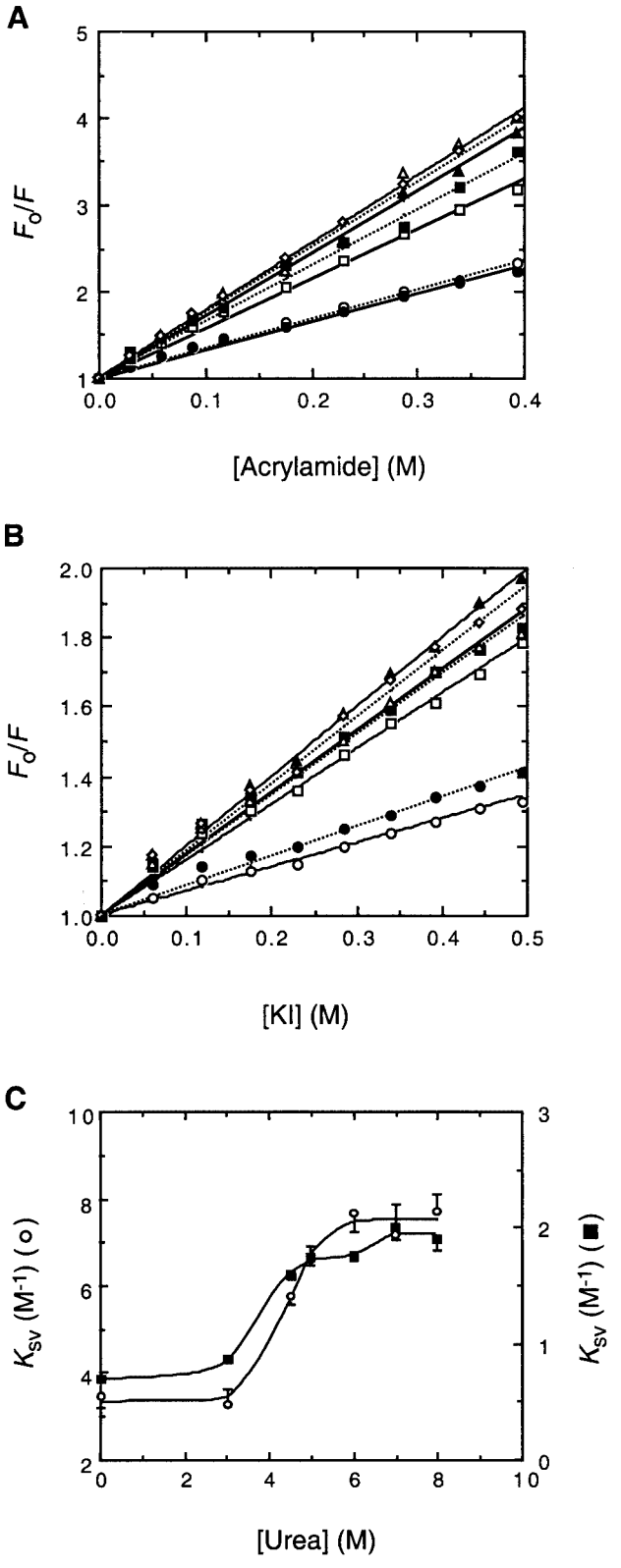

FIGURE 7 Quenching of the intrinsic fluorescence of human placental alkaline phosphatase by acrylamide or KI. Human placental alkaline phosphatase (12.9 μg/ml) in Tris-acetate buffer (0.1 M, pH 7.5) was denatured with 0 (○), 3.0 (●), 4.5 (□), 5.0 (■), 6.0 (△), 7.0 (▲), or 8.0 M (◇) urea at 30°C for 24 h. The denatured enzymes were then mixed with increasing amounts of acrylamide (*A*) or KI (*B*) and the fluorescence spectra of the enzyme were monitored. The integration area of the fluorescence emission spectrum between 330 and 360 nm was calculated. The excitation wavelength was set at 295 nm. The dilution and inner filter effects were corrected. (*C*) Stern-Volmer collisional quenching constants (K_{sv}) versus urea concentration plot. The quenching constants (○, from acrylamide quenching; ●, from KI quenching) were obtained from the linear regression analysis of the data shown in *A* and *B* according to the Stern-Volmer equation (Eq. 2). The curves in *C* were the fitted results according to a two-state or three-state unfolding mechanism ($N = 4$).

spectively. On the other hand, bis-ANS molecules bound more weakly to the denatured enzyme than the native enzyme, and the K_d values were 5.4 ± 0.9 μM and 16.0 ± 4.0 μM for the native- and 8-M urea-denatured enzymes, respectively.

Quaternary structure of human placental alkaline phosphatase during urea denaturation

Human placental alkaline phosphatase is a homodimeric protein. Our previous experimental results clearly indicated that GdnHCl-induced denaturation of the enzyme is biphasic in nature (Hung and Chang, 1998). The biphasic phenomenon is a simultaneous dissociation-denaturation process. Because the dissociation and denaturation occurred simultaneously, it was not possible to clearly distinguish between these two processes.

The molecular weight of the equilibrium-denatured enzyme in various concentrations of urea was examined by sucrose-density gradient ultracentrifugation under denaturing conditions. The enzyme existed as dimers in the absence of denaturant (Fig. 10 *A*) and dissociated during urea denaturation (Fig. 10). The dimeric enzyme was ~80% dissociated at urea concentration of 6 M, where the fluorescence or CD signals have not reached a maximum (Figs. 1–4). The results cannot differentiate dissociation and denaturation as separate steps during urea denaturation.

DISCUSSION

The detailed mechanism that directs the primary structure of a polypeptide chain to fold into the correct biologically active enzyme is a challenging question and has raised much discussion (cf. Aurora et al., 1997; Beasley and Hecht, 1997; Brockwell et al., 2000; Dill, 1997, 1999; Fedorov and Baldwin, 1997; Ruddon and Bedows, 1997; Tsai et al., 1999). Several models for the mechanism of protein folding have been proposed. The simple sequential model postulates a unique folding pathway with defined and sequential intermediates. More recently, the model of ensembles and funnel landscapes has attracted much attention (Baldwin, 1995; Dill, 1999; Dill and Chan, 1997; Tsai et al., 1999). On one hand, the folding of small proteins may be rapid with no detectable intermediates, conforming to a

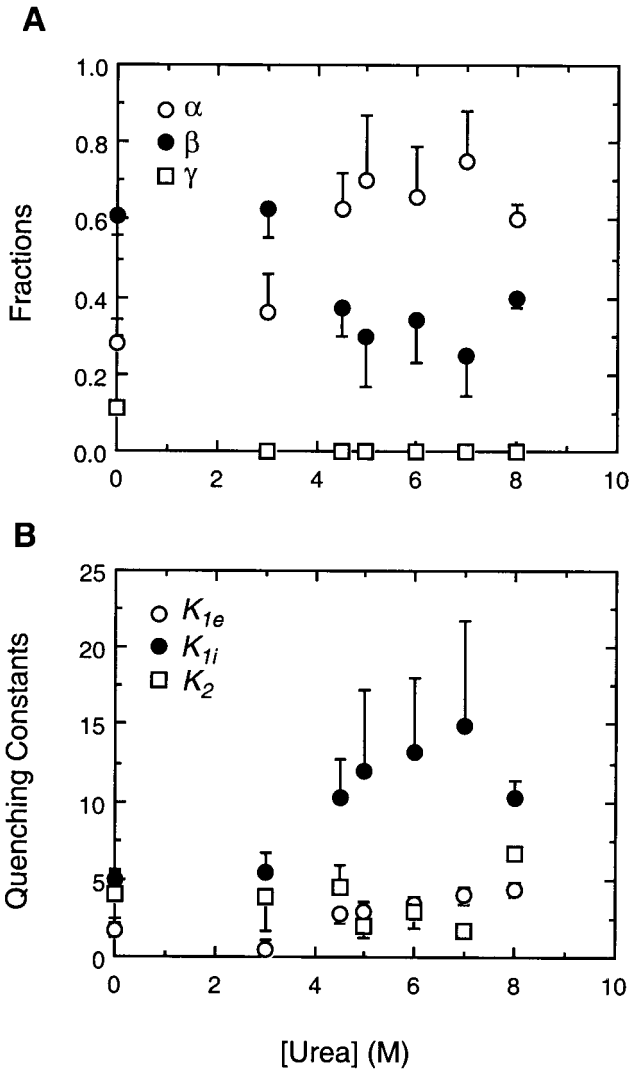

FIGURE 8 Variations of the fraction of accessible groups and quenching constants of the urea-denatured human placental alkaline phosphatase toward the nonselective or the selective quenchers accessed by double quenching of the intrinsic fluorescence of the enzyme by acrylamide and KI. Human placental alkaline phosphatase (12.9 μg/ml) in Tris-acetate buffer (0.1 M, pH 7.5) was denatured with 0 to 8 M urea at 30°C for 24 h. KI (0–0.3 M) was added into the assay mixture. The denatured enzymes containing various concentrations of KI were then mixed with increasing amounts of acrylamide. The emission spectrum areas among 330 to 360 nm were calculated. The excitation wavelength was set at 295 nm. The dilution and inner filter effects were corrected. The data were computer analyzed according to Eq. 3. (*A*) α, β, and γ, which represent the external, internal, and nonquenchable fluorophors of total fraction fluorophors, were used in analyzing the unfolding process. (*B*) Variations of external (K_{1e}) and internal (K_{1i}) quenching constants for acrylamide and quenching constant for KI (K_2) in urea denaturation ($N = 2$).

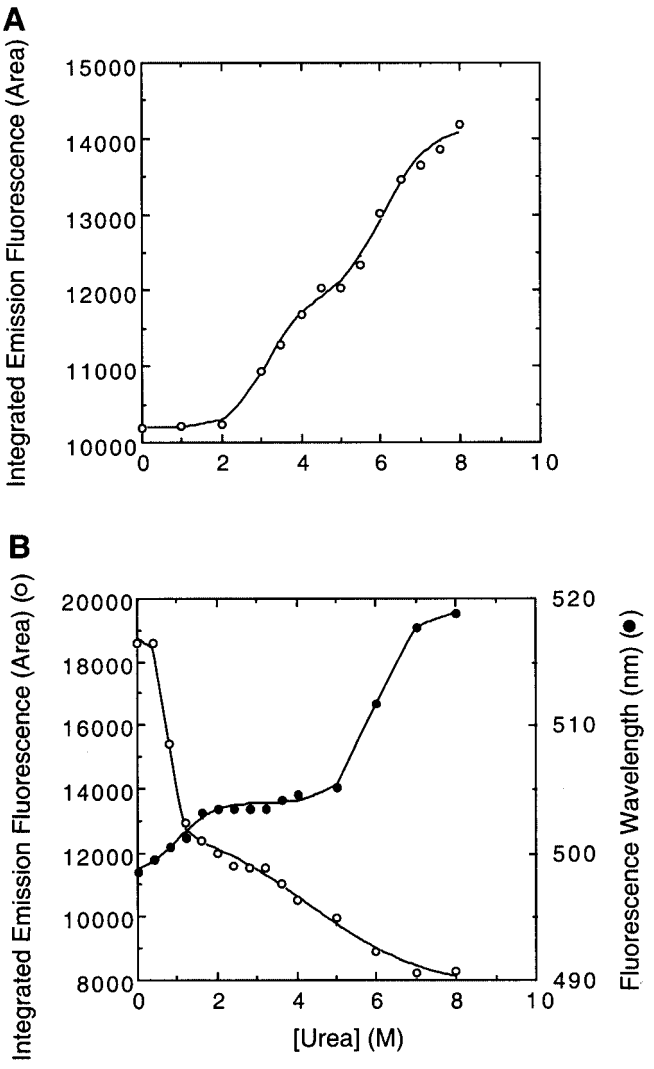

FIGURE 9 Binding of ANS and bis-ANS to the urea-denatured human placental alkaline phosphatase. Human placental alkaline phosphatase (12.9 μg/ml) in Tris-acetate buffer (0.1 M, pH 7.5) was denatured with various concentrations of urea at 30°C for 24 h and the fluorescence emissions were measured after ANS or bis-ANS addition. (*A*) ANS fluorescence of the urea-denatured alkaline phosphatase. The excitation wavelength was set at 370 nm, and the integrated area of the fluorescence emission spectrum between 420 and 560 nm was calculated. The final concentration of ANS was 40.0 μM. (*B*) bis-ANS fluorescence of urea-denatured alkaline phosphatase. The excitation wavelength was set at 395 nm. The final concentration of bis-ANS was 4.0 μM. These data were fitted to three-state unfolding model ($N = 3$). (○) Integrated emission fluorescence area; (●) fluorescence wavelength shift.

smooth funnel energy landscape (cf. Huang and Oas, 1995; Schindler et al., 1995; Sosnick et al., 1994). Large proteins or proteins that consist of several structural domains, on the other hand, may show multiple intermediates during the folding process reflected in a rugged funnel landscape (for reviews, see Bai and Englander, 1996; Fink et al., 1998; Jaenicke, 1996; Jennings and Wright, 1993; Kim and Baldwin, 1990; Privalov, 1996; Sugawara et al., 1991).

Folding and assembly of alkaline phosphatase in vitro and in vivo have been intensively investigated due to differential stability of this enzyme from various sources (Akiyama and Ito, 1993; Cioni et al., 1989; Hoylaerts and Millán, 1991; Mersol et al., 1993; Miggiano et al., 1987;

TABLE 2 Binding of ANS or bis-ANS to the urea-unfolding human placental alkaline phosphatase*

Urea concentration (M)	ANS		Bis-ANS	
	ΔF_{max}	K_d (μM)	ΔF_{max}	K_d (μM)
0	577.0 ± 81.9	165.4 ± 29.8	916.3 ± 51.3	5.4 ± 0.9
1.0	–†	–	615.8 ± 61.0	8.9 ± 1.5
2.0	760.5 ± 106.5	153.3 ± 25.9	–	–
3.0	792.4 ± 101.4	144.1 ± 22.5	561.4 ± 59.5	10.6 ± 1.8
4.5	843.5 ± 122.3	136.5 ± 23.5	547.3 ± 62.4	13.1 ± 2.2
5.0	875.6 ± 129.6	132.4 ± 24.2	539.7 ± 61.0	15.3 ± 2.4
6.0	893.4 ± 79.5	132.2 ± 14.4	519.3 ± 61.3	14.7 ± 2.4
7.0	903.3 ± 69.6	118.9 ± 11.5	516.9 ± 102.4	16.8 ± 4.0
8.0	949.9 ± 70.3	111.7 ± 10.5	486.8 ± 93.5	16.0 ± 4.0

*The ΔF_{max} and K_d values for the ANS and bis-ANS binding were calculated according to Eq. 4 ($N = 3$).
†Not detected.

Sarkar and Ghosh, 1996; Subramaniam et al., 1995). We have focused here on characterizing the equilibrium unfolding in chemical denaturants to delineate the thermodynamic stability of the placental alkaline phosphatase. In this paper, we show that the reversible unfolding/refolding of human placental alkaline phosphatase in urea definitely involves multiple equilibrium unfolding/folding intermediate states, which implies differential conformational stability among

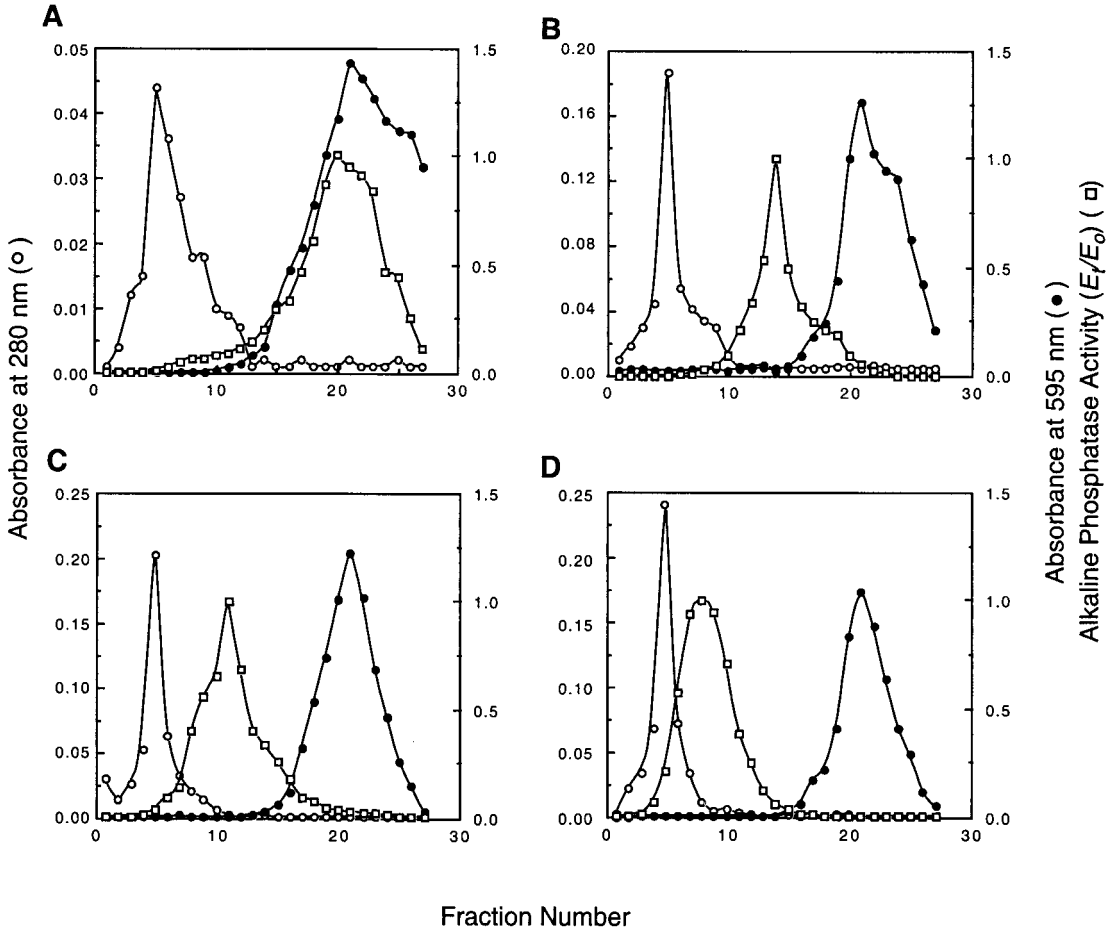

FIGURE 10 Sucrose-density gradient ultracentrifugation of the urea-denatured human placental alkaline phosphatase. The enzyme was denatured with various concentrations of urea in Tris-acetate buffer (0.1 M, pH 7.5) and ultracentrifuged in a 5 to ~20% sucrose-density gradient at 6500 × g for 19 h to separate the dimeric and monomeric enzyme molecules. (*A* to *D*) Urea concentrations of 0, 2.0, 4.0, and 6.0 M, respectively. ○, Bovine serum albumin (2 mg, molecular weight 67,000); ●, β-galactosidase (0.1 mg, molecular weight 116,000); □, placental alkaline phosphatase (63 μg) ($N = 2$).

the subdomains of the enzyme. The non-coincidence of the unfolding curves for enzyme intrinsic fluorescence (Figs. 1–3), CD spectroscopy (Fig. 4), the quenching experiments for accessibility of fluorophors (Fig. 8), the ANS and bis-ANS binding to the hydrophobic region of the enzyme (Fig. 9), together with enzymatic activity changes (Fig. 6) all demonstrate that there are indeed multiple unfolding/refolding intermediates entrapped during urea unfolding process. At least six transitions were detected by various structural probes. The midpoints of these transitions were 0.4 to 2.6 M, 3.1 to 4.1 M, 4.3 to 5.4 M, 5.2 to 5.6 M, 6.0 to 6.6 M, and 7.1 to 8.5 M urea, respectively, in the minimal unfolding sequence shown in Scheme 1.

Human placental alkaline phosphatase is a dimeric enzyme and has four tryptophan residues in each monomer. The overall structure of placental alkaline phosphatase is similar to the *E. coli* enzyme (Kim and Wyckoff, 1991; Murphy et al., 1995) and has a basic three-layer ($\alpha\beta\alpha$) sandwich architecture with a central 10-stranded β-sheet flanked by 15 helices and another three-stranded β-sheet, along with coils and loops (Fig. 11). The placental enzyme is characterized by a crown domain, an additional N-terminal helix, and another metal-binding domain (Le Du et al., 2001). The active site region is located at the upper part of the central β-sheet, containing the Zn1-Zn2-Mg metal triplet that is important for maintaining the rigidity of the protein interior as well as for catalysis (Stec et al., 2000; Hung and Chang, 2001). Each monomer of the enzyme can be divided into several domains. The core 10-stranded β-sheet constitutes the rigid central sheet domain II. The surrounding helical and coiled structures are divided into two parts. The N-terminal part constitutes domain I, which also contains the minor three-stranded β-sheet as well as the crown domain and the N-terminal helix characteristic of the placental enzyme. This domain is extensively involved in the subunit association in the dimeric enzyme. The C-terminal region constitutes domain III. Correlation of these structures to conformational stability is revealed by sensitivity of the enzyme to chemical denaturants.

Tryptophanyl fluorescence or phosphorescence has been demonstrated to be excellent structural probe for *E. coli* alkaline phosphatase (Cioni et al., 1989; Mersol et al., 1991, 1993; Strambini, 1987; Subramaniam et al., 1995; Sun et al., 1997). The four Trp in the placental enzyme are 100% conserved in mammals but not in bacteria. Trp-168 and Trp-237 are located in the coil and helix regions, respectively, of the C-peripheral domain, whereas Trp-248 is located at the side of the central β-sheet region. Trp-12 is located at the large N-terminal helix. The even distributions of the four Trp in placental alkaline phosphatase make Trp fluorescence an excellent probe for monitoring the structural changes of the enzyme (Fig. 11). Analysis of the accessibility of these Trp by the SwissPDB Viewer (Guex and Peitsch, 1997) indicates the following accessibility order: Trp-12 > Trp-248 > Trp-168 > Trp-237. The K_m of the substrate was not changed at urea concentrations up to 8 M (Fig. 6 *C*). This is consistent with the polypeptide chain flexibility information shown in Fig. 11 *B*. The active center is located at a rigid region of the molecule.

The importance of metal ions and the phosphate ion in the structural stability of *E. coli* alkaline phosphatase had been examined by Janeway et al. (1993). Placental alkaline phosphatase has an extra structural metal ion in addition to the Zn1-Zn2-Mg1 catalytic triad. We have demonstrated previously that the placental alkaline phosphatase is stabilized in GdnHCl-denaturation in the presence of 1 mM phosphate and 10 mM $MgCl_2$. The $[GdnHCl]_{0.5}$ increased from 1.66 M for the Mg-free enzyme to 2.95 M for the Mg-phosphate containing enzyme (Hung and Chang, 2001). Removing the tightly bound zinc ions from the enzyme by exhaustive dialysis with nitriloacetic acid resulted in an enzymatically inactive enzyme form, which had a different conformation as detected by fluorescence quenching (Hung and Chang, 2001). The multiple conformations detected in the enzyme with various metal contents strongly suggest the involvement of metal ions in stabilization of some parts of the structural integrity.

The quaternary structure of the enzyme was quite stable. The urea unfolding of the enzyme was a simultaneous dissociation-unfolding process. The x-ray structure of placental alkaline phosphatase explains the extra-stability of the quaternary structure of the placental enzyme. There are extensively entangled structures at the monomer-monomer interface. The interactions between two monomers are remarkable, e.g., C-terminal loop at the bottom and the large crown domain on the top of each monomer wind around each other; the long N-terminal helix on the bottom also extends deeply into another monomer. Substitution of a single amino acid of the bacteria alkaline phosphatase at the interface region sacrifices not only the integrity of the assembled dimer but also the stability of the monomer fold (Martin et al., 1999). This situation is even more pronounced in the mammalian placental enzyme, which has two large domains at the interface region. For this reason, it is conceivable that folded monomers cannot be separated, even at a high concentration of chemical denaturants. Molecular weight determination by sucrose density gradient ultracentrifugation indicated that the quaternary structure of the enzyme is quite stable in urea, and the fluorescence signal is insensitive to protein concentration in the enzyme amounts used in most of the experiments (12.9 μg/ml). Folded monomeric species do not exist at any equilibrium. In this extreme case, the energetics can be treated in manners similar to that for a monomeric protein unfolding process (Cai and Schirch, 1996; Neet and Timm, 1994), albeit multiple unfolding intermediates might be involved in multidomain proteins. The second transition of enzyme activity change, which has a midpoint at 6.5 M urea, might be attributed to the dissociation of the subunits. This conclusion is supported by the fitting results shown in Fig. 1 *A*.

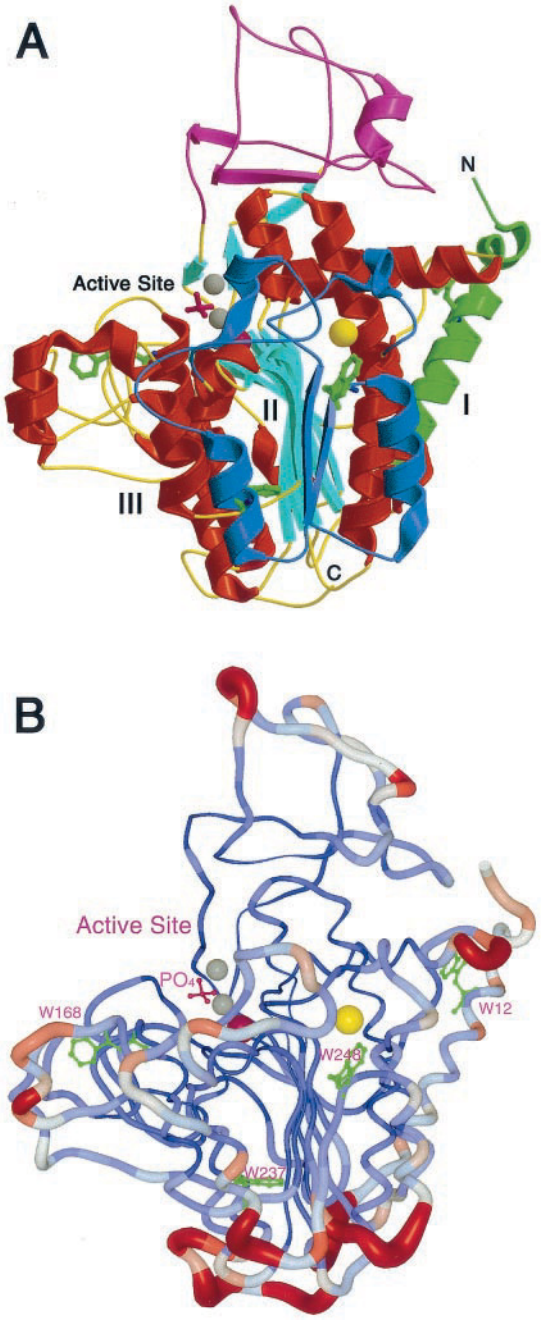

FIGURE 11 Structural features of human placental alkaline phosphatase. (*A*) The structure of placental alkaline phosphatase (pdb code: 1ew2) clearly indicates the basic $\alpha\beta\alpha$ folding pattern, designated as domains I, II, and III, respectively. The active site region is located at the top of the central 10-stranded β-sheet, highlighted with the bound phosphate (*purple*) and the Zn1-Zn2-Mg3 metal triplet region (large balls in *gray* and *violet*, respectively). The four Trp residues (W12, W168, W237, and W248) are presented in green ball-and-stick. Comparing with the bacterial alkaline phosphatase, the structural features of the placental enzyme include a crown domain on top (*purple*), a N-terminal helix (*green*), and an additional metal binding domain (*blue*), which contributed additional components to the $\alpha\beta\alpha$ main structure. The additional metal ion (Mg^{2+}) is shown as a *yellow* ball. (*B*) The structural flexibility of the enzyme is shown as a variable worm of the polypeptide chain. The rigid structure of the central β-sheets is shown as a thinner worm in blue. The more flexible peripheral regions are shown in red. Only one of the subunits is shown. This figure was generated with MOLSCRIPT (Kraulis, 1991) and rendered with Raster3D program (Merrit and Murphy, 1994).

At low enzyme concentrations, the missing transition thus may be assigned to the dissociation step, which is the second to last step in the unfolding pathway at higher protein concentrations (Table 1).

The properties of ANS and bis-ANS binding to the enzyme during urea unfolding are interesting because they show opposite results. As shown in Fig. 9 *A*, the ANS molecule prefers to bind to the denatured enzyme rather than to the native enzyme. However, the behavior of the bis-ANS molecule was just the opposite, preferring to bind with the native enzyme rather than to the denatured enzyme (Fig. 9 *B*). These observations may be attributed to the amphipathic nature of the ANS-type dyes (Lakowicz, 1999). The different binding behaviors of ANS and bis-ANS suggest that they might have entrapped different unfolding intermediates. The molecular weight of bis-ANS is 2-fold larger than ANS, and the two halves of bis-ANS molecule are perpendicular to each other (Arighi et al., 1998), which might cause some different steric effects and result in the opposite fluorescence change between ANS and bis-ANS.

In the present study, we provide conclusive evidence that demonstrates the multiple equilibrium unfolding/refolding intermediate states of the placental alkaline phosphatase. Because the unfolding and refolding follow the same pathway, the unfolding of placental alkaline phosphatase in urea seems to follow a sequential rather than a nonsequential pathway (Sánchez del Pino and Fersht, 1997). However, it is very difficult to assume the rate-limiting step of the sequential unfolding process from the free energy information, which vary substantially among different biophysical techniques. More recently, Dignam et al. (2001) also detected multiple unfolding intermediates of the glycyl-tRNA synthetase by the emission fluorescence spectral shift and places our work into a useful perspective. The novel part in the present case is that an unusually high number of intermediates were entrapped in vitro during urea unfolding process of human placental alkaline phosphatase. However, it should be pointed out that because relatively low and physiological concentrations of salt do cancel out many of the intermediates shown in Fig. 1 *A*, all these intermediates might not be involved in the normal in vivo folding environment of the enzyme inside the cell. With these caveats in mind, we try to interpret our data in terms of tertiary structure and energy landscape of the enzyme.

Because we have identified several discrete unfolding intermediates, the final landscape of the native enzyme should have a ragged surface. The peripheral domains are unfolded in the early stages of the unfolding process with

formation of some intermediates of nearly equal free energy. On the other hand, the central core structures are more stable and are the first parts to find their way in the landscape searching in the folding process. As demonstrated in Fig. 1 *C*, the fluorescence intensity of the enzyme at urea concentrations up to 9.5 M still did not reach a plateau, so the denatured state should not be regarded as a completely unfolded random coil. The folding pathway is hypothesized as follows: fusion of microdomain or building blocks forms the partially folded monomers, I_5. Association of two partially folded monomers results in the formation of partially folded dimers, I_4. The formation of intermediate form I_3 is followed by central domain annealing, which transforms to I_2 and I_1 states by incorporation of peripheral domains I and/or II, and then finally reaches the functional dimeric enzyme. In these intermediate macrostates, the enzyme molecules that have large degrees of freedom can have many conformations (microstates). In other words, any intermediate state does not mean a single trap in the energy funnel but represents an average over many microscopic conformations. This conclusion is corroborated by the fact that the active site of *E. coli* alkaline phosphatase can be reconstituted by a number of pathways (Sarkar and Ghosh, 1996).

This work was supported by the National Science Council, Republic of China (Frontiers in Sciences Program, grant NSC 89-2312-B016-001). We thank Daniel L. Floyd for reading the final version manuscript before publication. H.C.H. is a postdoctorate fellow awarded by the National Health Research Institute, Republic of China (RE90N001).

REFERENCES

Akiyama, Y., and K. Ito. 1993. Folding and assembly of bacterial alkaline phosphatase in vitro and in vivo. *J. Biol. Chem.* 268:8146–8150.

Arighi, C. N., J. P. Rossi, and J. M. Delfino. 1998. Temperature-induced conformational transition of intestinal fatty acid binding protein enhancing ligand binding: a functional, spectroscopic, and molecular modeling study. *Biochemistry.* 37:16802–16814.

Aurora, R., T. P. Creamer, R. Srinivasan, and G. D. Rose. 1997. Local interactions in protein folding: lessons from the alpha-helix. *J. Biol. Chem.* 272:1413–1416.

Bai, Y., and S. W. Englander. 1996. Future direction in folding: the multi-state nature of protein structure. *Proteins.* 24:145–151.

Baldwin, R. L. 1995. The nature of protein folding pathways: the classical versus the new. *J. Biomol. NMR.* 5:103–109.

Beasley, J. R., and M. H. Hecht. 1997. Protein design: the choice of de novo sequences. *J. Biol. Chem.* 272:2031–2034.

Brockwell, D. J., D. A. Smith, and S. E. Radford. 2000. Protein folding mechanisms: new methods and emerging ideas. *Curr. Opin. Struct. Biol.* 10:16–25.

Cai, K., and V. Schirch. 1996. Structural studies on folding intermediates of serine hydroxymethyltransferase using fluorescence resonance energy transfer. *J. Biol. Chem.* 271:27311–27320.

Calhoun, D. B., J. M. Vanderkooi, and S. W. Englander. 1983. Penetration of small molecules into proteins studied by quenching of phosphorescence and fluorescence. *Biochemistry.* 22:1533–1539.

Chang, T. C., S. M. Huang, T. M. Huang, and G. G. Chang. 1992. Human placental alkaline phosphatase: an improved purification procedure and kinetic studies. *Eur. J. Biochem.* 209:241–247.

Cioni, P., L. Piras, and G. B. Strambini. 1989. Tryptophan phosphorescence as a monitor of the structural role of metal ions in alkaline phosphatase. *Eur. J. Biochem.* 185:573–579.

Dawson, R. M. C., D. C. Elliott, W. H. Elliott, and K. M. Jones. 1986. Data for Biochemical Research, Third Ed. Clarendon Press, Oxford. 370.

Dignam, J. D., X. Qu, and J. B. Chaires. 2001. Equilibrium unfolding of *Bombyx moni* glycyl-tRNA synthetase. *J. Biol. Chem.* 276:4028–4037.

Dill, K. A. 1997. Additivity principles in biochemistry. *J. Biol. Chem.* 272:701–704.

Dill, K. A. 1999. Polymer principles and protein folding. *Protein Sci.* 8:1166–1180.

Dill, K. A., and H. S. Chan. 1997. From Levinthal to pathways to funnels. *Nature Struct. Biol.* 4:10–19.

Dobryszycki, P., K. Rymarezuk, G. Bulaj, and M. Rochman. 1999. Effect of acrylamide on aldolase structure: I. Induction of intermediate states. *Biochim. Biophys. Acta.* 1431:338–350.

Eftink, M. R. 1994. The use of fluorescence methods to monitor unfolding transitions in proteins. *Biophys. J.* 66:482–501.

Eftink, M. R., and C. A. Ghiron. 1981. Fluorescence quenching studies with proteins. *Anal. Biochem.* 114:199–227.

Fedorov, A. N., and T. O. Baldwin. 1997. Cotranslational protein folding. *J. Biol. Chem.* 272:32715–32718.

Fink, A. L., K. A. Oberg, and S. Seshadri. 1998. Discrete intermediates versus molten globule models for protein folding: characterization of partially folded intermediates of apomyoglobin. *Fold. Des.* 3:19–25.

Fishman, W. H. 1990. Alkaline phosphatase isozymes: recent process. *Clin. Biochem.* 23:99–104.

Guex, N., and M. C. Peitsch. 1997. SWISS-MODEL and the Swiss-Pdb Viewer: an environment for comparative protein modelling. *Electrophoresis.* 18:2714–2723.

Hoylaerts, M. F., and J. L. Millán. 1991. Site-directed mutagenesis and epitope-mapped monoclonal antibodies define a catalytically important conformational difference between human placental and germ cell alkaline phosphatase. *Eur. J. Biochem.* 202:605–616.

Huang, G. S., and T. G. Oas. 1995. Structure and stability of monomeric lambda repressor: NMR evidence for two-state folding. *Biochemistry.* 34:3884–3892.

Hung, H. C., and G. G. Chang. 1998. Biphasic denaturation of human placental alkaline phosphatase in guanidinium chloride. *Proteins.* 33: 49–61.

Hung, H. C., and G. G. Chang. 2001. Modulation of human placental alkaline phosphatase activity by slow binding of the magnesium or zinc ion at the M3 site of the enzyme. *Protein Sci.* 10:34–45.

Jaenicke, R. 1996. Protein folding and association: In vitro studies for self-organization and targeting in the cell. *Curr. Top. Cell. Regul.* 34:209–314.

Janeway, C. M. L., X. Xu, J. E. Murphy, A. Chaidaroglou, and E. R. Kantrowitz. 1993. Magnesium in the active site of *Escherichia coli* alkaline phopshatase is important for both structural stabilization and catalysis. *Biochemistry.* 32:1601–1609.

Jennings, P. A., and P. E. Wright. 1993. Formation of a molten globule intermediate early in the kinetic folding pathway of apomyoglobin. *Science.* 262:892–896.

Kim, E. E., and H. W. Wyckoff. 1991. Reaction mechanism of alkaline phosphatase based on crystal structure. *J. Mol. Biol.* 218:449–464.

Kim, P. S., and R. L. Baldwin. 1990. Intermediates in the folding reactions of small proteins. *Annu. Rev. Biochem.* 59:631–660.

Kraulis, P. 1991. MOLSCRIPT: a program to produce both detailed and schematic plots of protein structure. *J. Appl. Crystallogr.* 24:946–950.

Lakowicz, J. R. 1999. Principles of fluorescence spectroscopy, 2nd Ed. Kluwer/Plenum, New York. 237–289.

Le Du, M. H., T. Stigbrand, M. J. Taussig, A. Ménez, and E. A. Stura. 2001. Crystal structure of alkaline phosphatase from human placenta at 1.8 Å resolution: implication for a substrate specificity. *J. Biol. Chem.* 276:9158–9165.

Lehrer, S. S. 1971. Solute perturbation of protein fluorescence: the quenching of the tryptophanyl fluorescence of model compounds and of lysozyme by iodide ion. *Biochemistry.* 10:3254–3262.

Martin, D. C., S. C. Pastrarandis, and E. R. Kantrowitz. 1999. Amino acid substitution at the subunit interface of dimeric *Escherichia coli* alkaline phosphatase cause reduced structural stability. *Protein Sci.* 8:1152–1159.

McComb, R. B., G. N. Bowers, and S. Posen. 1979. Alkaline Phosphatases, Plenum Press, New York.

Merrit, E. A., and M. E. P. Murphy. 1994. Raster 3D version 2.0: a program for photorealistic molecular graphics. *Acta Crystallogr*. D50: 869–873.

Mersol, J. V., D. G. Steel, and A. Gafni. 1991. Quenching of tryptophan phosphorescence in *Escherichia coli* alkaline phosphatase by long-range transfer mechanisms to external agents in the rapid-diffusion limit. *Biochemistry.* 30:668–675.

Mersol, J. V., D. G. Steel, and A. Gafni. 1993. Detection of intermediate protein conformations by room temperature tryptophan phosphorescence spectroscopy during denaturation of *Escherichia coli* alkaline phosphatase. *Biophys. Chem.* 48:281–291.

Miggiano, G. A. D., A. Mordente, M. G. Pischiutta, G. E. Martorana, and A. Castelli. 1987. Early conformational changes and activity modulation induced by guanidinium chloride on intestinal alkaline phosphatase. *Biochem. J.* 248:551–556.

Morjana, N. A., B. J. McKeone, and H. F. Gilbert. 1993. Guanidine hydrochloride stabilization of a partially unfolded intermediate during the reversible denaturation of protein disulfide isomerase. *Proc. Natl. Acad. Sci. U.S.A.* 90:2107–2111.

Moss, D. W. 1992. Perspectives in alkaline phosphatase research. *Clin. Chem.* 38:2486–2492.

Murphy, J. E., T. T. Tibbitts, and E. R. Kantrowitz. 1995. Mutations at positions 153 and 328 in *Escherichia coli* alkaline phosphatase provide insight toward the structure and function of mammalian and yeast alkaline phosphatases. *J. Mol. Biol.* 253:604–617.

Nardini, M., and B. W. Dijkstra. 1999. α/β hydrolase fold enzymes: the family keeps growing. *Curr. Opin. Struct. Biol.* 9:732–737.

Neet, K. E., and D. E. Timm. 1994. Conformational stability of dimeric proteins: quantitative studies by equilibrium denaturation. *Protein Sci.* 3:2167–2174.

Ollis, D. L., E. Cheah, M. Cygler, B. Dijkstra, F. Frolow, S. M. Franken, M. Harel, S. J. Remington, I. Silman, J. Schrag, J. L. Sussman, K. H. G. Verschuren, and A. Goldman. 1992. The alpha/beta hydrolase fold. *Protein Eng.* 5:197–211.

Pace, C. N. 1986. Determination and analysis of urea and guanidine hydrochloride denaturation curves. *Methods Enzymol.* 131:266–280.

PetitClerc, C. 1976. Quantitative fractionation of alkaline phosphatase isoenzymes according to their thermostability. *Clin. Chem.* 22:42–48.

Privalov, P. L. 1996. Intermediate states in protein folding. *J. Mol. Biol.* 258:707–725.

Ruddon, R. W., and E. Bedows. 1997. Assisted protein folding. *J. Biol. Chem.* 272:3125–3128.

Sakiyama, T., J. C. Robinson, and J. Y. Chou. 1979. Characterization of alkaline phosphatases from human first trimester placentas. *J. Biol. Chem.* 254:935–938.

Sánchez del Pino, M. M., and A. R. Fersht. 1997. Nonsequential unfolding of the alpha/beta barrel protein indole-3-glycerol-phosphate synthase. *Biochemistry.* 36:5560–5565.

Santoro, M. M., and D. W. Bolen. 1988. Unfolding free energy changes determined by the linear extrapolation method: I. Unfolding of phenylmethanesulfonyl α-chymotrypsin using different denaturants. *Biochemistry.* 27:8063–8068.

Sarkar, S. N., and N. Ghosh. 1996. Reversible unfolding of *Escherichia coli* alkaline phosphatase: active site can be constituted by a number of pathways. *Arch. Biochem. Biophys.* 330:174–180.

Schindler, T., M. Herrler, M. A. Marahiel, and F. X. Schmid. 1995. Extremely rapid protein folding in the absence of intermediates. *Nature Struct. Biol.* 2:663–673.

Somogyi, B., S. Papp, A. Rosenberg, I. Seres, J. Matko, G. R. Welch, and P. Nagy. 1985. A double-quenching method for studying protein dynamics: separation of the fluorescence quenching parameters characteristic of solvent-exposed and solvent-masked fluorophors. *Biochemistry.* 24:6674–6679.

Sosnick, T. R., L. Mayne, R. Hiller, and S. W. Englander. 1994. The barriers in protein folding. *Nature Struct. Biol.* 1:149–156.

Sreerama, N., and R. W. Woody. 2000. Estimation of protein secondary structure from circular dichroism spectra: comparison of CONTIN, SELCON, and CDSSTR methods with an expanded reference set. *Anal. Biochem.* 287:252–260.

Stec, B., K. M. Holtz, and E. R. Kantrowitz. 2000. A revised mechanism for the alkaline phosphatase reaction involving three metal ions. *J. Mol. Biol.* 299:1303–1311.

Strambini, G. B. 1987. Quenching of alkaline phosphatase phosphorescence by O_2 and NO: evidence for inflexible regions of protein structure. *Biophys. J.* 52:23–28.

Subramaniam, V., N. C. H. Bergenhem, A. Gafni, and D. G. Steel. 1995. Phosphorescence reveals a continued slow annealing of the protein core after reactivation of *Escherichia coli* alkaline phosphatase. *Biochemistry.* 34:1133–1136.

Sugawara, T., K. Kuwajima, and S. Sugai. 1991. Folding of staphylococcal nuclease A studied by equilibrium and kinetic circular dichroism spectra. *Biochemistry.* 30:2698–2706.

Sun, L., E. R. Kantrowitz, and W. C. Galley. 1997. Room temperature phosphorescence study of phosphate binding in *Escherichia coli* alkaline phosphatase. *Eur. J. Biochem.* 245:32–39.

Tsai, C. J., S. Kumar, B. Ma, and R. Nussinov. 1999. Folding funnels, binding funnels, and protein function. *Protein Sci.* 8:1181–1190.

Van Hoof, V. O., and M. E. De Broe. 1994. Interpretation and clinical significance of alkaline phosphatase isoenzyme patterns. *Crit. Rev. Clin. Lab. Sci.* 31:197–293.